Caenorhabditis elegans CES-1 Snail Represses *pig-1* MELK Expression To Control Asymmetric Cell Division

Hai Wei,*,[1] Bo Yan,*,[1,2] Julien Gagneur,†,[3,4] and Barbara Conradt*,[4]

*Center for Integrated Protein Science Munich – CIPSM, Department Biology II, Ludwig-Maximilians-University Munich, 82152 Planegg-Martinsried, Germany and †Gene Center Munich, Ludwig-Maximilians-University Munich, 81377 Munich, Germany

ABSTRACT Snail-like transcription factors affect stem cell function through mechanisms that are incompletely understood. In the *Caenorhabditis elegans* neurosecretory motor neuron (NSM) neuroblast lineage, CES-1 Snail coordinates cell cycle progression and cell polarity to ensure the asymmetric division of the NSM neuroblast and the generation of two daughter cells of different sizes and fates. We have previously shown that CES-1 Snail controls cell cycle progression by repressing the expression of *cdc-25.2* CDC25. However, the mechanism through which CES-1 Snail affects cell polarity has been elusive. Here, we systematically searched for direct targets of CES-1 Snail by genome-wide profiling of CES-1 Snail binding sites and identified >3000 potential CES-1 Snail target genes, including *pig-1*, the ortholog of the oncogene maternal embryonic leucine zipper kinase (MELK). Furthermore, we show that CES-1 Snail represses *pig-1* MELK transcription in the NSM neuroblast lineage and that *pig-1* MELK acts downstream of *ces-1* Snail to cause the NSM neuroblast to divide asymmetrically by size and along the correct cell division axis. Based on our results we propose that by regulating the expression of the MELK gene, Snail-like transcription factors affect the ability of stem cells to divide asymmetrically and, hence, to self-renew. Furthermore, we speculate that the deregulation of MELK contributes to tumorigenesis by causing cells that normally divide asymmetrically to divide symmetrically instead.

KEYWORDS Snail-like transcription factor; ChIP-seq; maternal embryonic leucine zipper kinase (MELK); asymmetric cell division; *Caenorhabditis elegans*

SNAIL-LIKE zinc-finger transcription factors are critical for animal development and their deregulation has been implicated in tumorigenesis and metastasis (Barrallo-Gimeno and Nieto 2009; Puisieux *et al.* 2014; Nieto *et al.* 2016). The best-known function of Snail-like transcription factors is their role in orchestrating epithelial-mesenchymal transitions (EMTs), which are essential for development. Through EMTs, epithelial cells are converted into mesenchymal cells, which lack apico-basal polarity but have migratory properties, and thus contribute to the formation of various tissues and organs. In this context, Snail-like transcription factors directly repress the transcription of genes required for

apico-basal polarity and cell adhesion and thereby promote the induction of EMT. Snail-like transcription factors have also been shown to regulate fundamental processes such as cell proliferation and cell survival in animals as diverse as nematodes and mammals (Metzstein and Horvitz 1999; Yan *et al.* 2013; Puisieux *et al.* 2014). Recently, Snail-like transcription factors have also been implicated in various aspects of stem cell function (Guo *et al.* 2012; Desgrosellier *et al.* 2014; Hwang *et al.* 2014; Lin *et al.* 2014; Horvay *et al.* 2015; Ye *et al.* 2015; Tang *et al.* 2016). There is mounting evidence that in stem cell lineages, Snail-like transcription factors can promote not only self-renewal and, hence, the maintenance of an undifferentiated state, but also cell fate specification and, hence, the acquisition of a differentiated state. How the functions of Snail-like transcription factors in stem cell lineages are controlled, and through what mechanisms Snail-like transcription factors affect various aspects of stem cell function, remains largely unknown.

In *Caenorhabditis elegans*, the function of the Snail-like transcription factor CES-1 has been studied in the neurosecretory motor neuron (NSM) neuroblast lineage. About 410 min after the first cleavage of the *C. elegans* zygote, the NSM neuroblast

(NSMnb) divides asymmetrically by size and fate and gives rise to a larger daughter, the NSM, which differentiates into a serotonergic motor neuron, and a smaller daughter, the NSM sister cell (NSMsc), which dies within ∼20 min (Sulston *et al.* 1983). The gene *ces-2* encodes a bZIP transcription factor similar to the mammalian Hepatic Leukemia Factor (HLF) and acts as a negative regulator of *ces-1* Snail expression in the NSM neuroblast lineage (Metzstein *et al.* 1996; Metzstein and Horvitz 1999; Hatzold and Conradt 2008). Loss-of-function (lf) mutations of *ces-2* HLF or a gain-of-function (gf) mutation of *ces-1* Snail (*n703*gf) cause the NSMnb to divide symmetrically to give rise to two daughter cells of similar sizes (Ellis and Horvitz 1991; Hatzold and Conradt 2008). [The *n703*gf mutation is located in a *cis*-regulatory region of the *ces-1* gene and, as shown for *ces-2*(lf) mutations, presumably causes the mis- or overexpression of the *ces-1* gene in the NSM neuroblast lineage (Metzstein and Horvitz 1999; Hatzold and Conradt 2008).] In addition, presumably as a result of redundantly acting factors, the loss of *ces-1* does not appear to cause defects in the NSM neuroblast lineage; however, the loss of *ces-1* does suppress defects in the NSM neuroblast lineage caused by the loss of *ces-2* HLF (Ellis and Horvitz 1991) Moreover, rather than dividing along the ventral-lateral to dorsal-medial axis, in *ces-2* lf or *ces-1* gf animals, the NSMnb divides along different axes (Hatzold and Conradt 2008). Furthermore, a weak lf mutation of the gene *cya-1*, which encodes *C. elegans* Cyclin A, prevents the division of some NSMnbs, and this effect is greatly enhanced by the loss of *ces-2* or by *ces-1*(*n703*gf) (Yan *et al.* 2013). Therefore, it has been proposed that in the NSMnb, *ces-1* Snail coordinates cell polarity and cell cycle progression to allow the NSMnb to divide asymmetrically along the appropriate axis. Finally, *ces-1* Snail affects cell cycle progression in the NSMnb by directly repressing the transcription of the *cdc-25.2* gene, which encodes a *C. elegans* CDC25 phosphatase protein (Kim *et al.* 2010; Yan *et al.* 2013). The mechanism through which *ces-1* Snail affects cell polarity in this lineage is currently unknown.

In this study, we report results from our analysis of CES-1 Snail ChIP-seq data, which were acquired as part of the modENCODE project (Gerstein *et al.* 2010). Genome-wide profiling of CES-1 Snail binding sites identifies >3000 potential target genes in mixed-stage *C. elegans* embryos. In addition, gene ontology analysis of potential CES-1 Snail target genes confirms known and predicts novel functions of CES-1 Snail. Furthermore, we investigate the function of one potential CES-1 Snail target gene, the gene *pig-1*, which encodes an AMP-activated protein kinase (AMPK)-related protein kinase most similar to maternal embryonic leucine zipper kinase (MELK). We find that *pig-1* MELK acts downstream of *ces-1* Snail to cause the NSMnb to divide asymmetrically by size and along the correct axis.

Materials and Methods

ChIP-Seq data processing and analysis

The raw sequencing files of the CES-1 ChIP-seq experiments were obtained from the modENCODE website (DCCid;

modENCODE 3857). The alignment and all analyses were based on *C. elegans* genome WS220. Raw sequencing data from CES-1 ChIP-seq experiments were mapped to the *C. elegans* genome using bowtie2 (Langmead and Salzberg 2012). For each sample, the numbers of total and mapped reads are shown in Supplemental Material, Table S1. After mapping reads to the genome, peak calling algorithm MACS2 (Zhang *et al.* 2008) was used to identify regions of ChIP enrichment. Each biological repeat and corresponding control was used as treatment and control, respectively. The following parameters were used to predict CES-1 binding sites: qvalue (minimum FDR) cutoff 0.01 and mfold "5,50." MACS2 reported the summit, localization, and fold change of each binding site (peak). To measure the consistency from replicated experiments and identified reproducible binding sites, the IDR (irreproducible discovery rate) was calculated between the two repeats as described (Li *et al.* 2011). Only the reproducible binding sites (IDR cut-offs 0.1) were used for subsequent analysis. To show the concordance of the two repeats, correlation analysis was performed for the fold change of each pair of reproducible peaks (Figure 2A). The reproducible peaks from the two repeats were merged for downstream analysis.

The potential target genes of CES-1 were identified using the following criteria: if a merged peak is located in the transcription unit or within the 5′ promoter region (2 kb upstream of transcription start site) of a gene, this gene was defined as a potential target. The potential target genes were used for gene ontology (GO) analysis using DAVID6.8 (Huang da *et al.* 2009) at biological level 4. The overrepresented GO terms of CES-1 were compared with the overrepresented GO terms of 10 additional transcription factors (embryonic stage) (PHA-4, NHR-2, BLMP-1, ELT-3, LIN-13, CEH-39, GEI-11, MED-1, CES-1, MEP-1, LSY-2) (Table S3). The potential targets of these transcription factors were predicted using the same criteria based on the peaks reported by the modENCODE pipeline. The interpreted data files (gff3) containing the binding sites for each transcription factor were downloaded from modENCODE database (http://www.modencode.org).

Strains and genetics

All *C. elegans* strains were maintained at 20° as described in Brenner (1974). Bristol N2 was used as the wild-type strain. The following mutations and transgenes were used: LGI: *ces-1* (*n703*gf) *ces-1*(*n703 n1434*) (Ellis and Horvitz 1991), *ces-1*(*tm1036*) (Yan *et al.* 2013), *ces-2*(*bc213*) (Hatzold and Conradt 2008); LGII: *bcSi50* (P*_{ces-1}ces-1*::*yfp*) (this study), *bcSi43* (P*_{pig-1}gfp*) (this study), *ltIs202* (P*_{spd-2}gfp*::*spd-5*) (Woodruff *et al.* 2015); LGIII: *bcIs66* (P*_{tph-1}his-24*::*gfp*) (Yan *et al.* 2013); LGIV: *pig-1*(*gm344*) (Cordes *et al.* 2006), *pig-1*(*tm1510*) (National BioResource Project; https://shigen.nig.ac.jp/c.elegans/); and LGV: *ltIs44* (P*_{pie-1}mCherry*::*ph*^*PLCδ*) (Audhya *et al.* 2005).

Molecular biology

Plasmid pBC1531 (P*_{pig-1}gfp*) was generated using Gibson cloning. Briefly, using the primer pairs Ppig-1 vec F and Ppig-1

gfp R, Ppig-1 gfp F and gfptbb2gb R, and gfp tbb-2utr F and 4BP-SpeI-tbb-2 r' UTR, three DNA fragments (*pig-1* promoter/ 5' upstream region, *gfp* and *tbb-2* 3'UTR) were generated and combined using the primers Ppig-1 vec F and 4BP-SpeI-tbb-2 r' UTR. The resulting full-length fragment was then cloned into MosSCI vector pCFJ350 (Frokjaer-Jensen *et al.* 2012) sites AvrII and SpeI using T4 ligase to generate plasmid pBC1531 (P*pig-1gfp*). Plasmid pBC1448 (P*ces-1ces-1*::*yfp*) was generated by digesting the full-length *ces-1* rescuing fragment from pBC510 (Hatzold and Conradt 2008) using ApaI and SmaI enzymes, and inserting this fragment into MosSCI vector pCFJ350.

Transgenic animals

Germline transformations were performed as described in Mello and Fire (1995). For the generation of the P*pig-1gfp* MosSCI lines, plasmid pBC1531 was injected at a concentration of 10 ng/µl with the co-injection markers pCFJ601 at 50 ng/µl, pGH8 at 10 ng/µl, pCFJ90 at 2.5 ng/µl, and pCFJ104 at 5 ng/µl into the Universal MosSCI strain EG8079 (Frokjaer-Jensen *et al.* 2014) and integrated (single copy) on chromosome II to generate *bcSi43*. For the generation of the P*ces-1ces-1*::*yfp* MosSCI line, plasmid pBC1448 was injected at a concentration of 10 ng/µl with the co-injection markers pCFJ601 at 50 ng/µl, pGH8 at 10 ng/µl, pCFJ90 at 2.5 ng/µl, and pCFJ104 at 5 ng/µl into the MosSCI strain EG6699 (Frokjaer-Jensen *et al.* 2012) and integrated (single copy) on chromosome II to generate *bcSi50*.

Phenotypic analyses and microscopy

The number of surviving NSMsc was determined in L4 larvae using the *bcIs66* (P*tph-1his-24*::*gfp*) transgene as described in Yan *et al.* (2013). NSM and NSMsc volume and the position and orientation of the NSMnb division were analyzed using the *ltIs44* (P*pie-1mCherry*::*ph*$^{PLC\delta}$) transgene essentially as described (Chakraborty *et al.* 2015). The orientation of the NSMnb cleavage plane was additionally analyzed using *ltIs44* in combination with the *ltSi202* (P*spd-2 gfp*::*spd-5*) transgene, with which the position of the two centrosomes prior to cell division can be observed. Imaging was performed as follows. Embryos were imaged using a Leica TCS SP5 II confocal microscope. For all confocal imaging, the laser power setting was kept constant. Before confocal recording, all strains were incubated at 20° overnight. Six to ten adults were dissected to obtain mixed-stage embryos and embryos were mounted on 2% agar pads. Slides were sealed with petroleum jelly to avoid drying out and incubated at 25° until the embryos reached the comma stage of development. For all reporters, a Z-stack of 8–8.5 µm with a step size of 0.5 µm was used to record the NSMnb and its two daughter cells. Recording was started before NSMnb division and continued postcytokinesis. For determining "Dorsal-lateral/2nd cell volume ratio" and the orientation of the NSMnb cleavage plane, a noise reduction function was applied using the Leica Application Suite (LAS) software to remove background. To determine the cell volume of the NSM and the NSMsc, the ventral-medially located NSM and the dorsal-laterally located NSMsc

were identified by following the division of the NSMnb. After completion of cytokinesis, for every Z-slice, a region of interest (ROI) was drawn around the cell boundary of either the NSM or the NSMsc, the area of the ROI was determined for every Z-slice, and all areas of a certain cell summed up to obtain an estimate of the cell volume. The "Dorsal-lateral/2nd cell volume ratio" was determined by dividing the volume of the daughter located dorsal-laterally (the NSMsc and its derivatives) by the volume of the 2nd daughter (the NSM and its derivatives). The expression of the *bcSi43* (P*pig-1gfp*) transgene was quantified in the NSMnb before division using the *ltIs44* (P*pie-1mCherry*::*ph*$^{PLC\delta}$) transgene to mark the boundary of the NSMnb cell membrane. Quantification of *bcSi43* expression was performed on raw confocal images. Following confocal acquisition, for every Z-slice in which a distinct cell boundary of the NSMnb could be seen, the intensity of GFP fluorescence within the cell boundary was determined by drawing a ROI. The intensities of GFP fluorescence obtained for all Z-slices of a certain cell (six Z-slices) were summed up to obtain the total GFP fluorescence intensity of that particular cell. Total GFP fluorescence intensity was then divided by the total area of the ROI in the six Z-slices of that cell to obtain GFP concentration (fluorescence intensity/µm^2). The same procedure was used to determine GFP concentration in animals carrying the *bcSi43* (P*pig-1gfp*) transgene in Z3 (p4a). The mean "GFP concentration" of background signal obtained from a control strain only carrying the *ltIs44* (P*pie-1mCherry*::*ph*$^{PLC\delta}$) transgene (1.7 fluorescence intensity/µm^2) was too low to influence the GFP concentration of +/+, *ces-1*(*n703gf*), +/+[1], *ces-1*(*tm1036*), and +/+[2] during recordings. The same confocal laser power setting was used for the control and all experimental strains (+/+, *ces-1*(*n703gf*), +/+[1], *ces-1*(*tm1036*), and +/+[2]).

Data availability

Results

To systematically identify CES-1 Snail binding sites in the *C. elegans* genome, we analyzed ChIP-seq (chromatin immuno-precipitation combined with massively parallel DNA sequencing) data that had been generated as part of the modENCODE Project (Gerstein *et al.* 2010). As previously described, for ChIP-seq experiments, the modENCODE Project used stable transgenic *C. elegans* lines, each of which carries a transgene (for example, P*ces-1ces-1*::*gfp* referred to as "*wgIs174*") that mediates the synthesis of a specific, GFP-tagged *C. elegans* transcription factor (*i.e.*, CES-1::GFP) under the control of its endogenous promoter and *cis*-regulatory regions (Sarov *et al.* 2006, 2012). Chromatin bound by GFP-tagged protein was precipitated using an anti-GFP antibody and subjected to Illumina-based sequencing following the

modENCODE pipeline (Zhong *et al.* 2010). The nonprecipitated chromatin, which represents the total genomic DNA (input), was used as control. As starting material for CES-1::GFP ChIP-seq experiments, the modENCODE project used mixed-stage embryos. Finally, we obtained the *wgIs174* transgene and confirmed that it is expressed in appropriate cells during embryogenesis, such as cells of the developing pharynx (Figure S1).

Identification and characterization of CES-1 Snail binding sites

The modENCODE project performed CES-1::GFP ChIP-seq experiments in two independent biological replicates (Repeat1 and Repeat2). This led to a data set of ~7 million total reads in each replicate (Table S1), which provides sufficient coverage for ChIP-seq experiments of *C. elegans* transcription factors (Landt *et al.* 2012). Here, we analyzed this data set following the ENCODE and modENCODE guidelines (Landt *et al.* 2012). The reads of the two biological replicates and the corresponding controls were aligned with the *C. elegans* genome (WS220) and subjected to peak calling using MACS2 (Zhang *et al.* 2008). The CES-1 binding sites (peaks) were visualized using Integrative Genomics Viewer (IGV) (Robinson *et al.* 2011). As shown for chromosome IV in Figure 1A, the two biological replicates generated highly similar binding profiles. The reproducibility of the data was assessed by estimating the IDR between the replicates (Landt *et al.* 2012). Applying FDR (false discovery rate; calculated and reported by MACS2) and IDR cut-offs of ≤0.01 and ≤ 0.1, respectively, we identified 3417 reproducible CES-1 binding sites. Furthermore, for reproducible peaks, we found that the fold change of CES-1 binding is highly correlative (Pearson correlation 0.83) (Figure 2A). In addition, for the majority of reproducible peaks, the peak summits obtained from the two replicates are located within 100 bp of each other (Figure 2B), which indicates good concordance between the replicates. For subsequent analyses, we used the "merged peak" of reproducible peaks, which is generated by combining each pair of reproducible peaks.

The majority of merged peaks have lengths in the range of 200–500 bp (Figure 2C). Using MEME-chip (Bailey *et al.* 2009), we determined motifs enriched in these merged peaks. One motif identified [CAGC(T/A)GC] is similar to the classical Snail binding site (CAGGTG) (Figure 3), which has previously been shown to function as a CES-1 binding site (Metzstein and Horvitz 1999; Thellmann *et al.* 2003; Reece-Hoyes *et al.* 2009). In addition, we identified two *de novo* motifs [AAT(T/G/C)(A/C/G)AAT and AGACG(C/G)AG], which are significantly enriched (Figure 3) and which have previously not been shown to act as CES-1 binding sites. Finally, we evaluated the locations of the CES-1 peaks relative to protein-coding transcripts and observed a small yet significant enrichment of CES-1 peaks within 2 kb of transcriptional start sites (TSS) (67 *vs.* 62% for spatially randomized peak positions, *P*-value ≤0.0001; Figure 2D).

### Identification of potential CES-1 Snail target genes

The proximity of a binding site to the promoter is currently the best indicator for functional relevance. According to WS220, the genome size of *C. elegans* is 100 megabases (Mb) and contains 20,389 protein-coding genes. Genes are often located <2 kb from each other, either on the same or opposite strands. Furthermore, in most cases, the *cis*-regulatory regions sufficient for proper gene expression lie within 2 kb upstream of the TSS (Reinke *et al.* 2013). Therefore, if a CES-1 peak is located within the transcription unit or within 2 kb upstream of the TSS of a gene, this gene can be considered a potential CES-1 target gene. Using these criteria, >80% of the CES-1 peaks have at least one potential target gene, and a total of 3199 genes are identified as potential CES-1 target genes (Table S2). Among these target genes are classical Snail targets such as the gene *hmr-1*, which encodes *C. elegans* E-cadherin, and *sax-7*, which encodes the *C. elegans* ortholog of the human cell adhesion transmembrane-receptor L1 CAM (Puisieux *et al.* 2014; Nieto *et al.* 2016).

Gene ontology analysis of potential CES-1 Snail target genes

We performed GO analysis using the NIH Database for Annotation, Visualization, and Integrated Discovery (DAVID) (Huang da *et al.* 2009) to identify the "biological processes" (at Level 4) that are enriched among potential CES-1 target genes. This identified "cell cycle process" and "programmed cell death" among the most highly enriched processes (Table S3) confirming results from previous studies of *ces-1* function (Ellis and Horvitz 1991; Thellmann *et al.* 2003; Yan *et al.* 2013) (see below). GO analysis also predicts novel functions of *ces-1* Snail. For example, CES-1 target genes are overrepresented in biological processes related to sexual differentiation, aging, nervous system development, and cell signaling. Furthermore, we selected 50 of the most highly enriched "biological processes" and assessed their enrichment among the potential target genes of 10 other *C. elegans* transcription factors for which embryonic ChIP-seq data sets are available from modENCODE (BLMP-1, CEH-39, ELT-3, GEI-11, LIN-13, LYS-2, NHR-2, MED-1, MEP-1, and PHA-4) (Figure 4 and Table S3). Broad GO terms that are related to animal development (such as "larval development," "embryo development," "system development," or "animal organ development") are enriched among the target genes of most of these transcription factors as expected due to the known importance of transcription factors during development. Compared to the other transcription factors, CES-1 shares more similarities with the FoxA transcription factor PHA-4, the homeodomain transcription factor CEH-39, and the zinc-finger transcription factor LIN-13, which act as organ identity factor (PHA-4), X chromosome-signal element (CEH-39), and cell fate regulator (LIN-13), respectively (Figure 4) (Horner *et al.* 1998; Melendez and Greenwald 2000; Gladden and Meyer 2007).

CES-1 Snail affects the ability of the NSMnb to divide asymmetrically; however, the target gene or genes of CES-1 Snail in
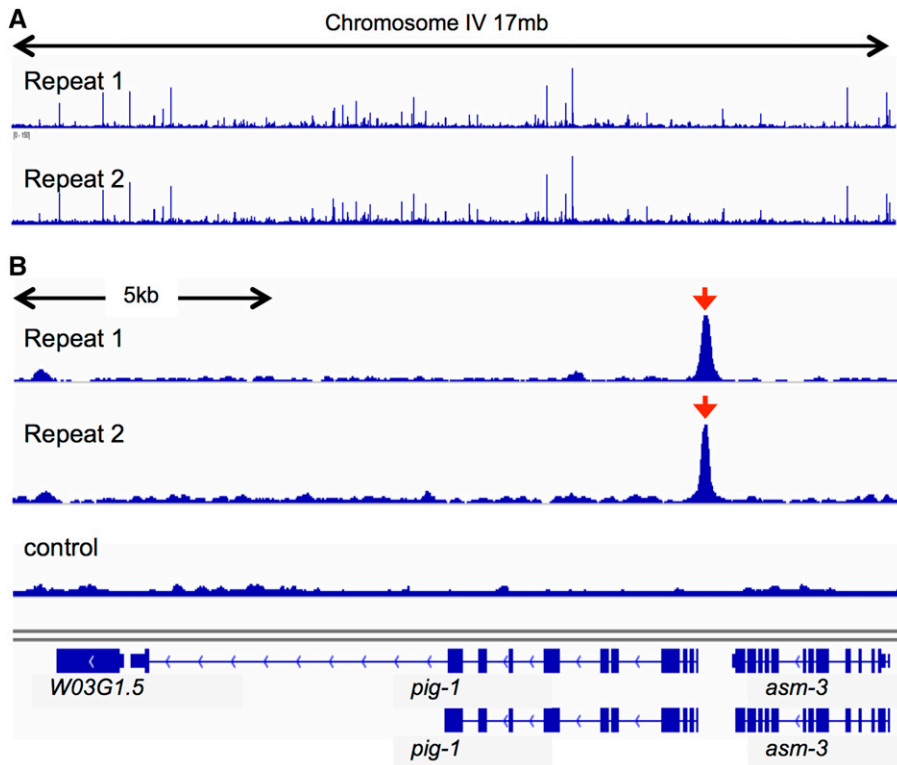
Figure 1 Visualization of CES-1 binding sites. CES-1 peaks from two biological replicates were predicted using MACS2 and visualized using IGV. (A) Overview of all CES-1 binding sites on chromosome IV. (B) Representative CES-1 binding sites in 20-kb region on chromosome IV that spans the *pig-1* locus. Red arrows point to the CES-1 binding sites.

this context are unknown. For this reason, we screened biological processes enriched among CES-1 Snail target genes for processes related to asymmetry and cell polarity and identified "asymmetric cell division" as highly enriched (enrichment of *P*-value 9.70E−04) (Table S3). Furthermore, among the target genes associated with "asymmetric cell division" (Table S5), we identified the gene *pig-1*, which is also associated with "programmed cell death" (enrichment of *P*-value 2.25E−18) (Table S4). *pig-1* encodes an AMP-activated protein kinase (AMPK)-related protein kinase most similar to MELK (Cordes *et al.* 2006; Ganguly *et al.* 2015). Interestingly, the *pig-1* MELK gene has previously been implicated in the asymmetric division of a number of *C. elegans* neuroblasts that divide to generate a smaller daughter that dies (Cordes *et al.* 2006) and in the programmed elimination of cells during *C. elegans* embryogenesis (Denning *et al.* 2012; Hirose and Horvitz 2013). Finally, the CES-1 Snail binding site profile revealed that there is a strong binding site just upstream of the TSS of the *pig-1* MELK gene (Figure 1B).

ces-1 Snail represses pig-1 MELK expression in the NSM neuroblast lineage

To test whether CES-1 Snail controls *pig-1* MELK expression in the NSM neuroblast lineage, we generated a transcriptional reporter in which the expression of the *gfp* gene is driven by an 850-bp fragment that spans bp −1 to bp −850 of the region immediately upstream of the *pig-1* TSS ($P_{pig-1}gfp$) (Figure 1B). (This 850-bp fragment covers the CES-1 binding site identified through ChIP-seq.) We generated a stable transgenic *C. elegans* line carrying a single copy of this reporter (MosSCI allele) and analyzed *gfp* expression in the

NSMnb. We found that in wild-type animals, *gfp* is expressed at a low level in the NSMnb (Figure 5, A and B; +/+). This level was reduced by ∼20% in animals homozygous for the *ces-1* gf mutation *n703*gf. To confirm that this decrease was specific to the presence of the *ces-1* gf mutation, we outcrossed this strain to remove *n703*gf (+/+[1]), and this brought the level of *gfp* expression back to that observed in the wild type. Furthermore, the level of *gfp* expression was increased by ∼25% in animals homozygous for the *ces-1* lf mutation *tm1036*, and outcrossing to remove *tm1036* (+/+[2]) confirmed that this increase is specific to the loss of *ces-1* (Figure 5, A and B). Finally, we analyzed *gfp* expression of the $P_{pig-1}gfp$ transgene in a second cell, Z3 (p4a). As shown in Figure S2, *gfp* expression in Z3 was not affected by the *ces-1* mutations. Based on these results, we conclude that *ces-1* Snail represses *pig-1* MELK transcription and, hence, *pig-1* MELK expression in the NSMnb.

pig-1 MELK is required for the correct position of the NSMnb cleavage plane

To determine whether *ces-1* Snail affects the asymmetric division of the NSMnb by acting through *pig-1* MELK, we analyzed the NSM neuroblast lineage in animals homozygous for strong lf mutations, *pig-1*(*gm344*) and *pig-1*(*tm1510*) (Cordes *et al.* 2006). [Both alleles are deletions that remove 524 bp (*gm344*; bp −381 to bp +143) or 1487 bp (*tm1510*; bp +178 to bp +1664) of the *pig-1* locus, respectively (Figure S3).] First, we analyzed the position of the cleavage plane during NSMnb division. In wild-type animals, the cleavage plane is shifted toward the dorsal-lateral side of the NSMnb (Sulston *et al.* 1983). Consequently, the NSMnb divides
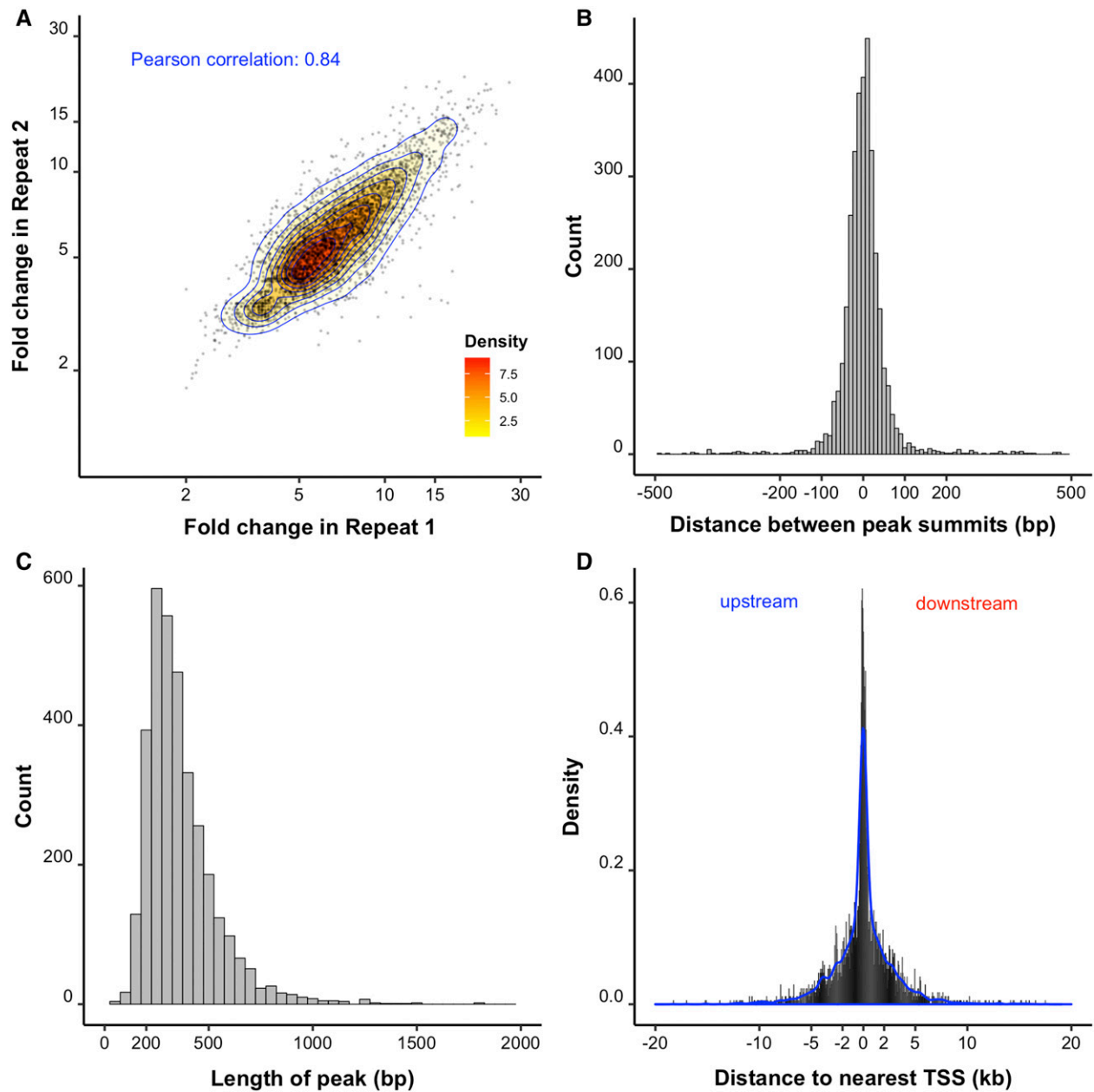
Figure 2 Characterization of CES-1 binding sites. CES-1 peaks were predicted using MACS2. (A) Density plot comparison between the fold change (fold enrichment for the peak summit against random Poisson distribution with local lambda, calculated by MACS2) of reproducible peaks from Repeat 1 and Repeat 2. Reproducible peaks from two biological replicates were identified using IDR cut-offs ≤0.1. Each dot represents a reproducible peak. Log 10 scale is used for *x* and *y* axis. (B) Distribution of the distances (in base pairs) between the summits of pairs of reproducible peaks. Reproducible peaks from two biological replicates were identified using IDR cutoff ≤0.1. (C) Distribution of the lengths (in base pairs) of the merged peaks. (D) Distribution of the distances (in kilobases) between CES-1 binding sites (peak summits of the merged peaks) and the TSS of the nearest protein-coding transcripts.

asymmetrically by size to give rise to a smaller daughter located dorsal-laterally, the NSMsc, and a larger daughter located ventral-medially, the NSM, with an average ratio of NSMsc to NSM volume of 0.69 (Figure 6). As shown below, mutations in *ces-2*, *ces-1*, and *pig-1* not only affect the position of the NSM cleavage plane, but also its orientation (Figure 7). However, regardless of the orientation of the cleavage plane, one cell (presumably the NSMsc) immediately moves into the dorsal-lateral position. For this reason, we determined the volume ratio of the two daughter cells by dividing the volume

of the daughter located dorsal-laterally by the volume of the other or "2nd" daughter (presumably the NSM) and refer to this ratio as "dorsal-lateral/2nd cell volume ratio" (Figure 6).

As shown previously, in animals homozygous for a lf mutation of *ces-2* (*bc213*) or the *ces-1* gf mutation *n703*gf, the NSMnb divides symmetrically with an average dorsal-lateral/2nd cell volume ratio of 1.05 and 1.08, respectively (Figure 6) (Hatzold and Conradt 2008). We found that in *pig-1*(*gm344*) or *pig-1*(*tm1510*) animals, the NSMnb also divides symmetrically with an average ratio of 1.04 and 1.03,
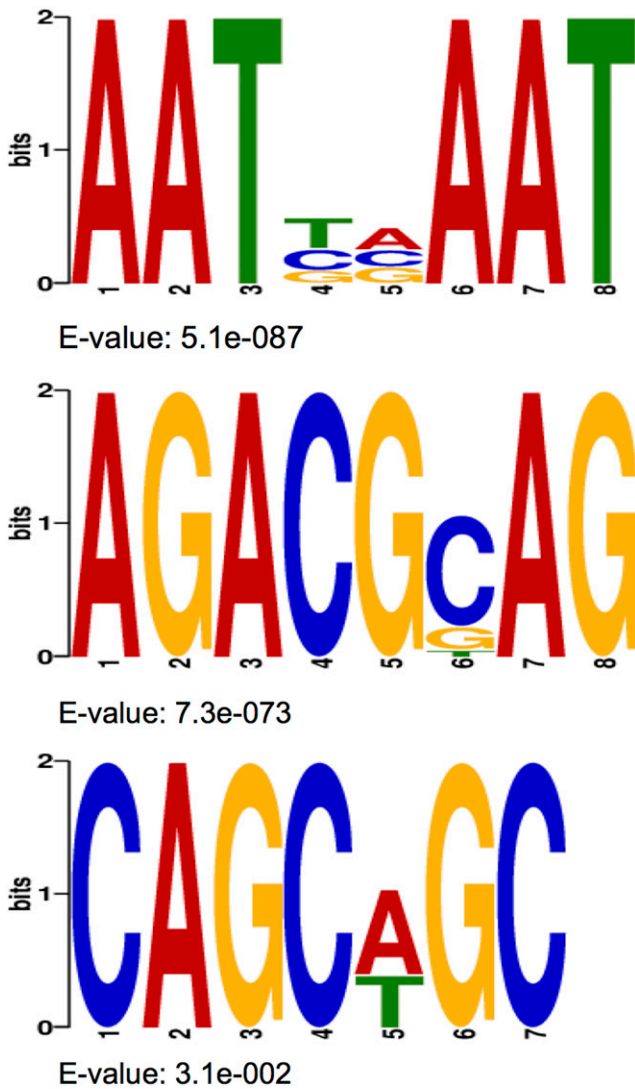
Figure 3 Motifs enriched in CES-1 peaks. Motifs enriched in CES-1 peaks (merged peaks from two biological repeats) were identified using MEME-chip. *E*-value represents fold enrichment. The last motif [CAGCA(T/A)G] is similar to the classic Snail binding site (CAGGTG).

respectively. Therefore, *pig-1* MELK is required for the ability of the NSMnb to divide asymmetrically by size. Furthermore, *ces-1* acts downstream of *ces-2* to affect NSMsc survival, and the loss of *ces-1* completely suppresses the defect in asymmetric NSMnb division observed in *ces-2*(*bc213*) animals (Figure 6) (Hatzold and Conradt 2008). In contrast, the loss of *ces-1* fails to suppress this defect in *pig-1*(*gm344*) animals, which indicates that in the NSMnb, *ces-1* Snail does not act downstream of *pig-1* MELK.

pig-1 MELK is required for the correct orientation of the NSMnb cleavage plane

Next, we analyzed the orientation of the cleavage plane during NSMnb division. In wild-type animals, the NSMnb divides along the ventral-lateral to dorsal-medial axis so that its daughter cells are positioned dorsal-laterally (NSMsc) and ventral-medially (NSM) (Figure 7). However, as previously

shown, in the majority of *ces-2*(*bc213*) or *ces-1*(*n703*gf) animals, different cleavage planes are observed (Figure 7) (Hatzold and Conradt 2008). We observed the same defect in the majority of *pig-1*(*gm344*) or *pig-1*(*tm1510*) animals, which demonstrates that *pig-1* MELK is also required for the polarization of the NSMnb and its ability to divide along the ventral-lateral to dorsal-medial axis. Interestingly, we also observed a defect in cleavage plane orientation in animals homozygous for the *ces-1* lf mutation *tm1036*. Specifically, in 44% of *ces-1*(*tm1036*) animals, the cleavage plane of the NSMnb was shifted by +90° (Type II cleavage) (Figure 7). [This specific shift was also observed in 27% of animals homozygous for another *ces-1* lf mutation, *n703 n1434* (Figure 7B).] Furthermore, the same +90° shift was observed in about half of *ces-1*(*tm1036*); *ces-2*(*bc213*) animals, confirming that *ces-1* is epistatic to *ces-2*. However, in both *pig-1*(*gm344*) animals and *ces-1*(*tm1036*); *pig-1*(*gm344*) animals, various cleavage planes other than the specific +90° shift were observed in the majority of animals (Figure 7B). Therefore, *pig-1* MELK is epistatic to *ces-1* Snail, which indicates that *pig-1* MELK acts downstream of *ces-1* Snail to affect the orientation and most likely also position of the NSMnb cleavage plane.

pig-1 MELK function in the NSM neuroblast is haploinsufficient

As described above, we found that *ces-1*(*n703*gf) reduces *gfp* expression of the P$_{pig-1}$*gfp* transgene by ~20% in the NSMnb whereas the *ces-1* lf mutation *tm1036* increases it by ~25%. This suggests that relatively small differences in the level of *pig-1* expression affect *pig-1* function in the NSMnb and cause a detectable phenotype. To test whether *pig-1* function in the NSMnb is haploinsufficient, we analyzed the position and orientation of the NSMnb cleavage plane in animals heterozygous for *pig-1*(*gm344*) [*pig-1*(*gm344*)/+]. As shown in Figure 6B and Figure 7B, we found that *pig-1*(*gm344*)/+ animals exhibit defects similar to the defects observed in homozygous *pig-1*(*gm344*) animals. Therefore, *pig-1* MELK function in the NSMnb is haploinsufficient.

The loss of pig-1 MELK has a modest effect on the cell death fate of the NSMsc

Apart from its roles in the NSMnb, *ces-1* Snail also plays a role in the daughters of the NSMnb. Immediately after NSMnb division, CES-1 Snail protein is detectable in the larger NSM, but not in the smaller NSMsc (Hatzold and Conradt 2008). The absence of CES-1 Snail in the NSMsc allows a heterodimer of HLH-2 and HLH-3 (HLH-2/HLH-3) (similar to the *Drosophila melanogaster* bHLH proteins, Daughterless and Achaete-scute, respectively) to activate transcription of the proapoptotic gene *egl-1* BH3-only and thereby trigger NSMsc death (Conradt and Horvitz 1998; Thellmann *et al.* 2003). In contrast, the presence of CES-1 Snail in the NSM blocks the ability of HLH-2/HLH-3 to activate *egl-1* BH3-only transcription and thereby causes NSM survival (Thellmann *et al.* 2003). In *ces-2* lf animals [and most probably in *ces-1*(*n703*gf) animals], CES-1 Snail protein is present in both
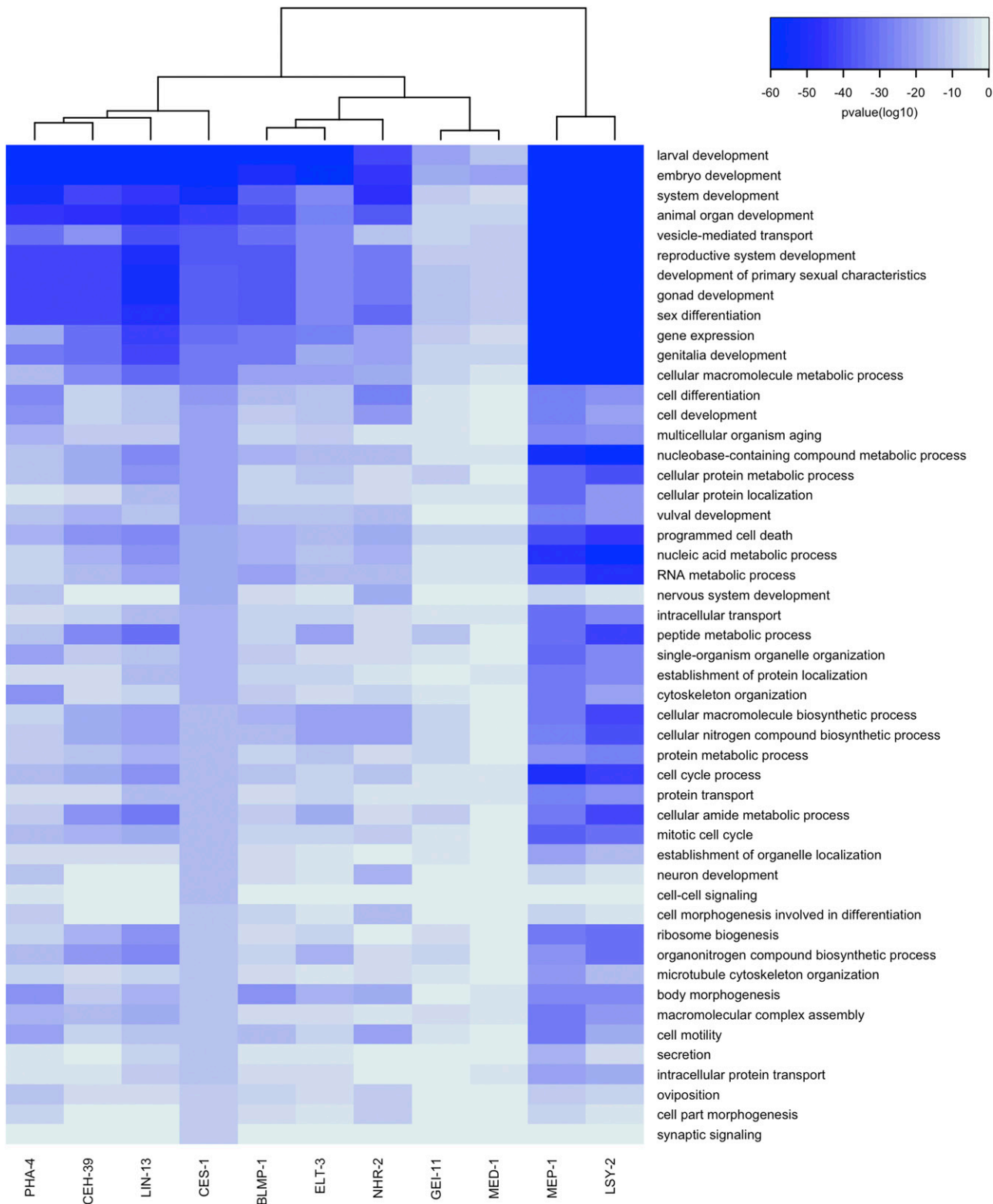
Figure 4 Gene ontology analysis. The potential target genes of PHA-4, NHR-2, BLMP-1, ELT-3, LIN-13, CEH-39, GEI-11, MED-1, CES-1, MEP-1, and LSY-2 were identified based on ChIP-seq experiments using *C. elegans* embryos as starting material that had been performed as part of the modENCODE project. GO analysis was performed at biological process Level 4 using DAVID. The overrepresented GO terms of CES-1 were ranked by *P*-value, and redundant GO categories were removed manually. The top 50 most highly enriched CES-1 GO terms were chosen for comparative GO study. The heat map shows the *P*-values (log 10) of these GO terms for the different transcription factors. The hierarchical clustering (performed based on the average agglomeration method) indicates the correlation between these transcription factors in embryos.
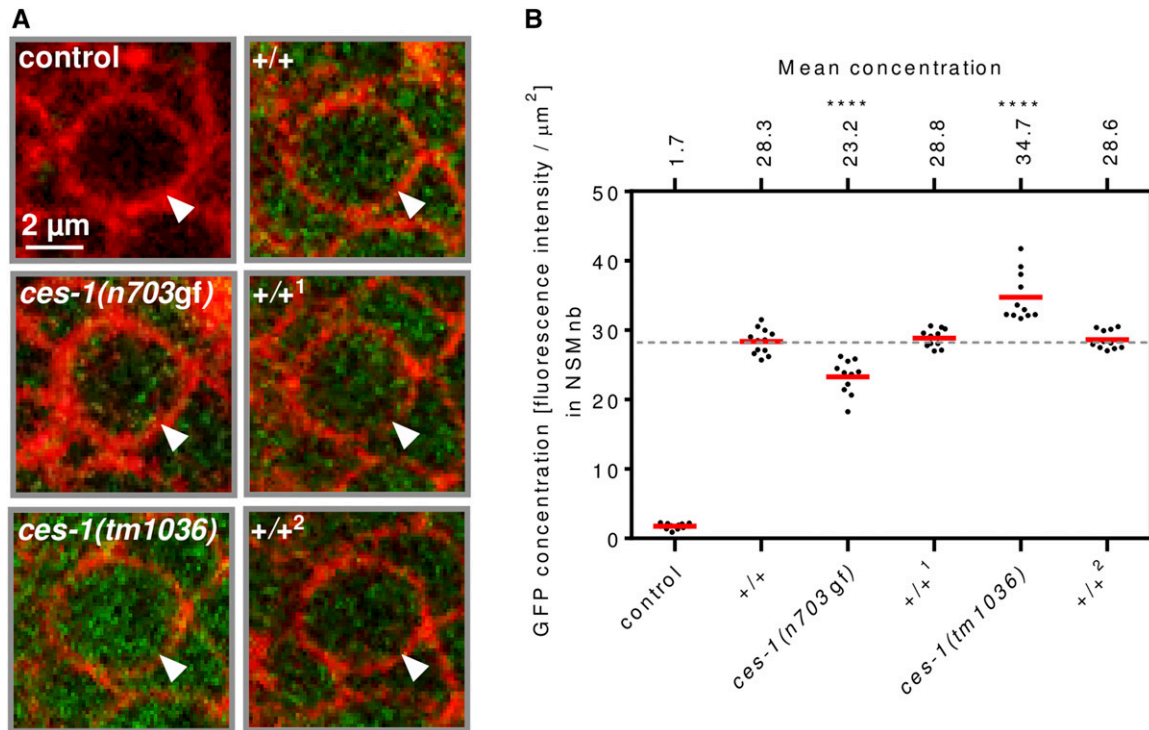
Figure 5 *ces-1* Snail represses *pig-1* MELK expression in the NSMnb. (A) Confocal images of representative NSMnbs at metaphase in control, wild-type (+/+, +/+[1], +/+[2]), *ces-1(n703gf)*, and *ces-1(tm1036)* animals. Control animals were transgenic for *ltIs44* ($P_{pie-1}mCherry::ph^{PLC\delta}$) transgene. Wild-type (+/+, +/+[1], +/+[2]), *ces-1(n703gf)*, and *ces-1(tm1036)* animals were transgenic for *bcSi43* ($P_{pig-1}gfp$) and *ltIs44* ($P_{pie-1}mCherry::ph^{PLC\delta}$) transgenes. +/+[1] indicates a strain from which *ces-1(n703gf)* was outcrossed. +/+[2] indicates a strain from which *ces-1(tm1036)* was outcrossed. White arrow heads indicate NSMnb. Bar, 2 μm. (B) GFP concentration [fluorescence intensity/μm²] in NSMnb in control animals (control) and in animals carrying the transgene $P_{pig-1}gfp$ (*bcSi43*) in various genetic backgrounds [+/+, *ces-1(n703gf)*, +/+[1], *ces-1(tm1036)*, +/+[2]] (*n* = 11–13). Each dot represents the GFP concentration in one NSMnb. Red horizontal lines indicate mean concentrations, which are stated on top. Gray dotted line indicates the mean concentration in wild type (+/+). Statistical significance was determined using the Student's *t*-test (**** $P \leq 0.0001$). All statistical analyses were done in comparison to wild type (+/+).

daughters after NSMnb division (Hatzold and Conradt 2008). Consequently, *egl-1* BH3-only transcription is repressed in both daughters and both daughters survive and differentiate into motor neurons (Ellis and Horvitz 1991; Thellmann *et al.* 2003). Therefore, in the NSMnb daughters, *ces-1* Snail is critically involved in the coordination of cell survival and cell fate specification.

To determine whether *pig-1* MELK also plays a role in cell survival and cell fate specification in the NSMnb daughters, we analyzed the effect of the loss of *pig-1* MELK on the fate of the NSMsc. In wild-type animals, the NSMsc dies (0% NSMsc survival); however, as previously shown (Ellis and Horvitz 1991; Hatzold and Conradt 2008), in *ces-2(bc213)* or *ces-1(n703gf)* animals, 80.6 or 97.4% of the NSMsc inappropriately survive, respectively (Figure 8A). We found that in *pig-1(gm344)* or *pig-1(tm1510)* animals, 2.1 or 1.2% of the NSMsc survived, respectively. Furthermore, while the loss of *ces-1* completely suppresses NSMsc survival in *ces-2(bc213)* animals (Ellis and Horvitz 1991; Hatzold and Conradt 2008), it had no effect on the modest NSMsc survival rate in *pig-1(gm344)* animals (Figure 8A), demonstrating that in the NSM neuroblast lineage, *pig-1* MELK acts downstream of *ces-1* Snail in the coordination of cell survival and cell fate specification as well.

Finally, we tested whether the loss of *pig-1* affects the kinetics of the NSMsc death. We found that in the wild type, from the time it is born, it takes the NSMsc an average of 21.9 min to become refractile and, hence, die (Figure 8, B and C). In contrast, in *pig-1(gm344)* or *pig-1(tm1510)* animals, it takes the NSMsc an average of 30.0 or 28.9 min, respectively, to become refractile and die. Therefore, while the loss of *pig-1* MELK only modestly affects the cell death fate of the NSMsc, it decreases the speed with which this fate is executed.

Discussion

Genome-wide profiling of DNA binding sites identifies novel functions of CES-1 Snail

The binding sites of the *D. melanogaster* Snail transcription factor have previously been identified using chromatin immuno-precipitation combined with microarray analysis (ChIP-on-chip) (Zeitlinger *et al.* 2007; Rembold *et al.* 2014). We analyzed data generated by the modENCODE Project for *C. elegans* CES-1 Snail using chromatin immuno-precipitation combined with massively parallel DNA sequencing (ChIP-seq) (Gerstein *et al.* 2010). Our analyses indicate that during embryonic development, *C. elegans* CES-1 Snail may contribute to the transcriptional regulation of >3000 genes. Among these genes
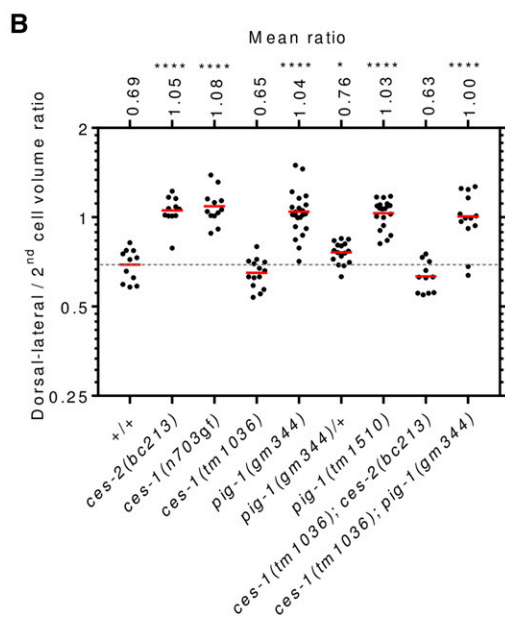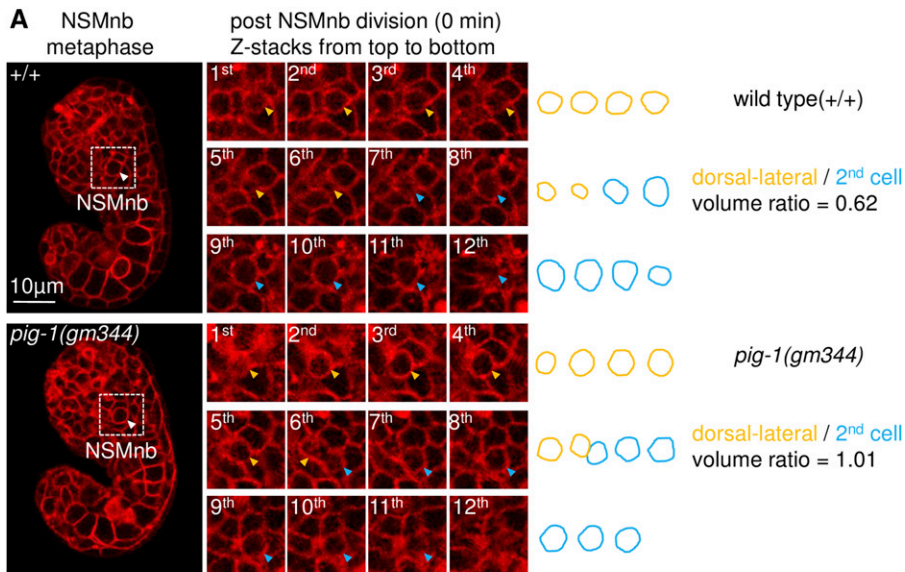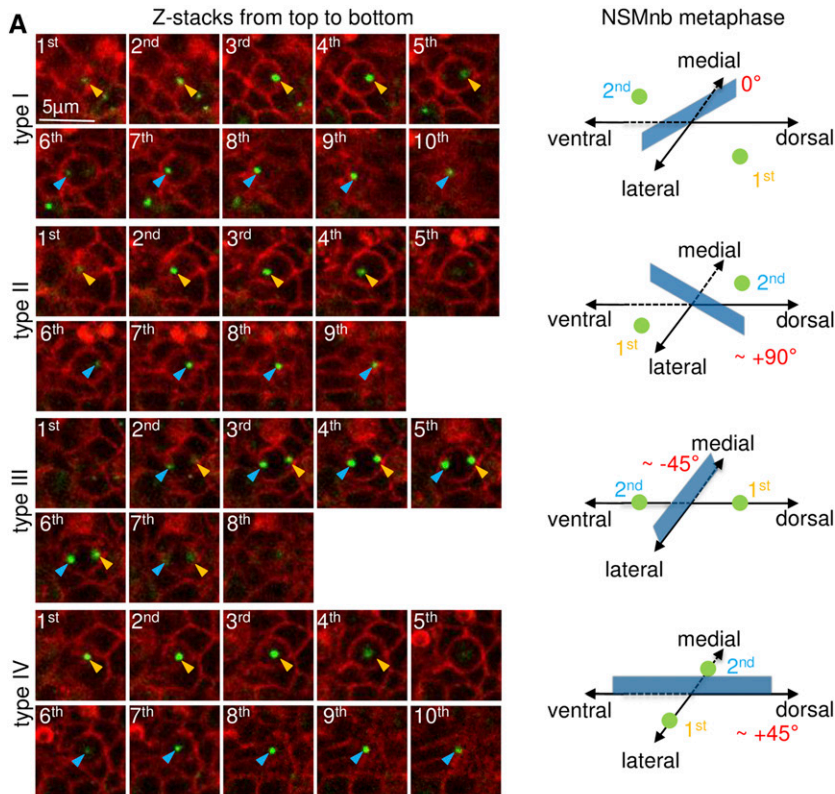
Figure 6 *pig-1* MELK is required for the correct position of the NSMnb cleavage plane. (A) (Left) Fluorescence images of representative wild-type (+/+) and *pig-1(gm344)* embryo carrying the transgene *ltIs44* (P_{pie-1}mCherry::$ph^{PLCδ}$). The white arrow points to the NSMnb, which is at metaphase. Bar, 10 μm. (Center) Representative series of eight consecutive confocal fluorescence images (Z-stacks, from top to bottom, 0.5-μm step size) of dorsal-lateral cell and 2nd cell immediately after the NSMnb divided in wild type (+/+) or *pig-1(gm344)*. The orange and blue arrows point to the dorsal-lateral cell or the 2nd cell, respectively. (Right) Schematic representations of the areas of the dorsal-lateral (orange) or 2nd cell (blue) in the consecutive images of the Z-stacks shown in the center and volume ratio of these two representative animals. (B) Volume ratio of dorsal-lateral daughter cell to 2nd daughter cell postcytokinesis in different genotypes [wild type (+/+), *ces-2(bc213)*, *ces-1(n703*gf), *ces-1(tm1036)*, *pig-1(gm344)*, *pig-1(gm344)/+*, *pig-1(tm1510)*, *ces-1(tm1036); ces-2(bc213)* and *ces-1(tm1036); pig-1(gm344)*] (n = 12–23). All strains were homozygous for the *ltIs44* (P_{pie-1}mCherry::$ph^{PLCδ}$) transgene. Each dot represents the ratio of one pair of daughter cells. Red horizontal lines represent the mean ratio obtained for a given genotype, which is stated on top. Gray dotted line indicates the +/+ mean ratio. Statistical significance was determined using the Student's *t*-test (* $P \leq 0.05$, **** $P \leq 0.0001$). All statistical analyses were done in comparison to wild type (+/+).

are genes whose orthologs in *D. melanogaster* and/or mammals are known targets of Snail-like transcription factors, confirming conservation among Snail-like transcription factors of fundamental functions, such as in the control of cell adhesion (Puisieux *et al.* 2014; Nieto *et al.* 2016). Gene ontology analysis of potential CES-1 target genes also reveals novel functions of CES-1 Snail; however, the actual contribution of *ces-1* Snail to these biological processes is currently unknown.

Two CES-1 Snail target genes have previously been described, the BH3-only gene *egl-1* and the CDC25 gene *cdc-25.2* (Thellmann *et al.* 2003; Yan *et al.* 2013). Interestingly, neither *egl-1* nor *cdc-25.2* are among the 3199 genes identified using the criteria that the CES-1 Snail binding site lies within the transcription unit or within 2 kb upstream of the TSS. In the case of *egl-1* BH3-only, CES-1 Snail binds to and acts through a conserved *cis*-regulatory element, which lies

∼3 kb downstream of the *egl-1* transcription unit (Thellmann *et al.* 2003). (There is a CES-1 Snail peak ∼2.5–4.0 kb downstream of *egl-1*, which may represent CES-1 Snail binding to region B.) In the case of *cdc-25.2*, a CES-1 Snail binding site is found ∼4.8–6.5 kb upstream of the TSS of *cdc-25.2* (Yan *et al.* 2013). Therefore, the CES-1 Snail binding sites in the *egl-1* and *cdc-25.2* loci are among the ∼20% of the 3417 binding sites that could not be assigned to a target gene using our criteria.

Our analysis of the sequences covered by CES-1 Snail peaks identified three motifs that are significantly enriched, among them a motif that is similar to the Snail binding site, which has been shown to function as a CES-1 binding site *in vitro*, in *C. elegans* and in the yeast one-hybrid system (Metzstein and Horvitz 1999; Thellmann *et al.* 2003; Reece-Hoyes *et al.* 2009). The two other motifs are more highly enriched and potentially represent novel CES-1 binding sites. Interestingly,

Figure 7 *pig-1* MELK is required for the correct orientation of the NSMnb cleavage plane. (A) (Left) Series of 8–10 consecutive confocal fluorescence images (0.5-μm step size) from top to bottom of Z-stacks of representative wild-type (type I) or *pig-1(gm344)* (type II–IV) animals exhibiting different orientations of the NSMnb cleavage plane and, hence, different types of cell divisions (type I–V). The orientation of the cleavage plane was determined based on the position of the centrosomes and the position of the daughter cells immediately after the completion of the NSMnb division. Orange arrows point to the centrosomes that segregate into the dorsal-lateral cell and blue arrows point to the centrosomes that segregate into the 2nd cell. All embryos analyzed were homozygous for the transgene *ltSi202* (P$_{spd-2}$::*gfp*::*spd-5*), which visualizes centrosomes, and for the transgene *ltIs44* (P$_{pie-1}$mCherry::ph^{PLCδ}), which labels the plasma membrane. Bar, 5 μm. (Right) Schematic representations of different cell division types (type I–IV) observed for the NSMnb in the animals shown left. Blue translucent rectangles represent cleavage planes of the NSMnb. Red numbers indicate the shifts (+ indicates clockwise shift, − indicates counterclockwise shift) relative to wild type (type I) (0°). (B) Percentage cell division types observed in different genotypes [wild type (+/+), *ces-2(bc213)*, *ces-1(n703*gf), *ces-1(tm1036)*, *ces-1(n703 01434)*, *pig-1(gm344)*, *pig-1(gm344)*/+, *pig-1(tm1510)*, *ces-1(tm1036)*; *ces-2(bc213)* and *ces-1(tm1036)*; *pig-1(gm344)*] (*n* = 14–19). All strains were homozygous for the *ltIs44* (P$_{pie-1}$mCherry::ph^{PLCδ}) transgene.
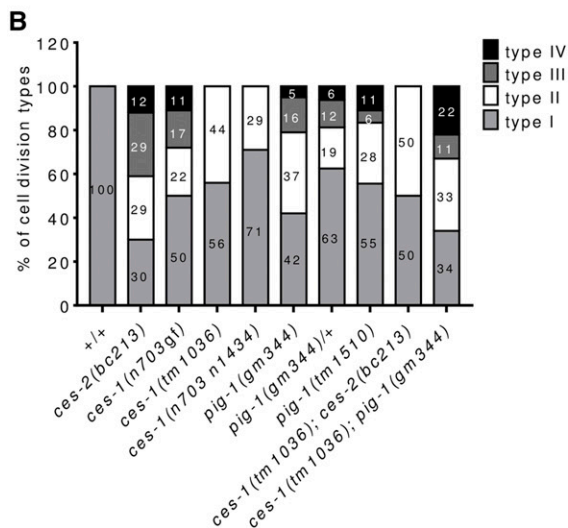
these two motifs differ from a motif that was recently identified for CES-1 Snail using protein-binding microarrays (CCTGTTG) (Narasimhan *et al.* 2015). For protein-binding microarrays, purified GST-tagged fusions of the DNA-binding domain of the transcription factor of interest plus 50 flanking amino acids are tested for "hybridization" to an array containing DNA probes each 35 bp in length. In contrast, for ChIP-seq, GFP-tagged, full-length CES-1 Snail protein is tested for binding to chromatin in *C. elegans* embryos (Gerstein *et al.* 2010). Hence, the different CES-1 Snail binding motifs identified might be a result of different experimental conditions.

ces-1 Snail affects the polarity of the NSMnb and its ability to divide asymmetrically by size by repressing pig-1 MELK expression

Among the potential CES-1 Snail target genes, we identified the gene *pig-1* MELK, which has previously been implicated in asymmetric cell division and the programmed elimination of cells during embryogenesis (Cordes *et al.* 2006; Denning *et al.* 2012; Hirose and Horvitz 2013). We demonstrate that *pig-1* MELK is required (in a haploinsufficient manner) for the correct position and orientation of the cleavage plane during the division of the NSMnb. Furthermore, we provide evidence that *pig-1* MELK acts downstream of CES-1 Snail and

A

Genotype	% NSMsc survival	n
+/+	0.0	190
ces-2(bc213)	80.6 ****	180
ces-1(n703gf)	97.4 ****	266
ces-1(tm1036)	0.0	264
pig-1(tm1510)	1.2*	110
pig-1(gm344)	2.1 **	280
ces-1(tm1036); ces-2(bc213)	0.0	202
ces-1(tm1036); pig-1(gm344)	2.0 **	196
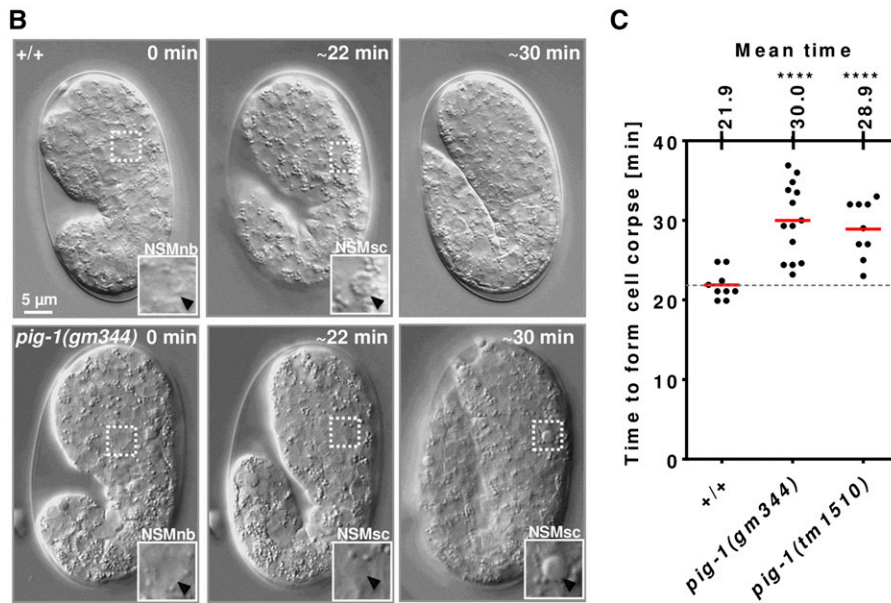
Figure 8 Loss of *pig-1* MELK affects the cell death fate of the NSMsc. (A) Percentage NSMsc survival in different genetic backgrounds [wild type (+/+), *ces-2(bc213)*, *ces-1(n703*gf), *ces-1 (tm1036)*, *pig-1(tm1510)*, *pig-1(gm344)*, *ces-1 (tm1036)*; *ces-2(bc213)* and *ces-1(tm1036)*; *pig-1(gm344)*]. All strains were homozygous for the *bcIs66* (P$_{tph-1}$*his-24*::*gfp*) transgene. *n* indicates the total number of NSMsc analyzed. Statistical significance was determined using the Student's *t*-test (* $P \leq 0.05$, ** $P \leq 0.005$, **** $P \leq 0.0001$). All statistical analyses were done in comparison to wild type (+/+). (B) Nomarski images of representative wild-type (+/+) and *pig-1(gm344)* embryos starting at NSMnb metaphase (0 min). Bar, 5 µm. In the wild type, the NSMsc is refractile and a cell corpse at ~22 min and can no longer be detected at ~30 min. In *pig-1(gm344)*, the NSMsc is refractile and a cell corpse at ~30 min. Insets show NSMnb and NSMsc. Black arrow heads point to relevant cells. (C) Quantification of the time it takes the NSMsc to form a cell corpse in wild-type (+/+), *pig-1(tm1510)*, and *pig-1(gm344)* animals. Each dot represents an individual NSMsc (*n* = 9–14). Red horizontal lines represent the mean time for a given genotype, which is stated on top. Gray dotted line indicates the mean time in wild type. Statistical significance was determined using the Student's *t*-test (**** $P \leq 0.0001$).

that CES-1 represses *pig-1* MELK transcription. Therefore, we propose that CES-1 Snail affects the polarization of the NSMnb and its ability to divide asymmetrically by repressing *pig-1* MELK expression (Figure 9A). Apart from blocking the death of the NSMsc, *ces-1(n703*gf) blocks the death of the IL2 sister cell (Ellis and Horvitz 1991). Interestingly, the loss of *pig-1* has been shown to affect the survival of the IL2 sister cell as well (Cordes *et al.* 2006). Therefore, *ces-1* Snail may also act through *pig-1* MELK to control the asymmetric division of the IL2 neuroblast.

The loss of *ces-2* or *ces-1(n703*gf) affect the position and orientation of the NSMnb cleavage plane as well as the fate of the NSMsc (Ellis and Horvitz 1991; Hatzold and Conradt 2008) (Figure 9B). The loss of *pig-1* MELK affects the position and orientation of the NSMnb cleavage plane, but has only a modest effect on NSMsc fate. [The fact that the loss of *pig-1* MELK has only a modest effect on NSMsc fate explains why *pig-1* was previously thought to not play a role in the NSM neuroblast lineage (Cordes *et al.* 2006).] The loss of *ces-2* and presumably also *ces-1(n703*gf) increases *ces-1* Snail expression, which, after NSMnb division, results in detectable levels of CES-1 Snail protein and repression of *egl-1* BH3-only transcription in

both daughter cells (Hatzold and Conradt 2008). In contrast, the loss of *pig-1* MELK does not increase *ces-1* Snail expression in the NSM neuroblast lineage (Figure S4). Therefore, we propose that NSMsc survival in *ces-2(bc213)* and *ces-1(n703*gf) animals is a result of the inappropriate presence and amount of CES-1 Snail in the NSMsc rather than the symmetric division along different cell division axes of the NSMnb *per se*. CES-1 Snail could also potentially have additional target genes that are required for the segregation of cell fate determinants, such as "apoptotic potential," during NSMnb division (Chakraborty *et al.* 2015) (Figure 9A).

Regulation of PIG-1 MELK activity through control of gene expression

The activity of AMPK-related protein kinases (of which MELK kinases form a subgroup) can be regulated by upstream kinases such as mammalian liver kinase B1 (LKB1) (Lizcano *et al.* 2004), which forms a complex with the proteins STRAD and MO25 (Alessi *et al.* 2006). Indeed, there is evidence that in asymmetric cell division and in the programmed elimination of cells, *pig-1* acts in a pathway that is also dependent on *par-4* and/or *strd-1* and *mop-25.2*, which encode *C. elegans*
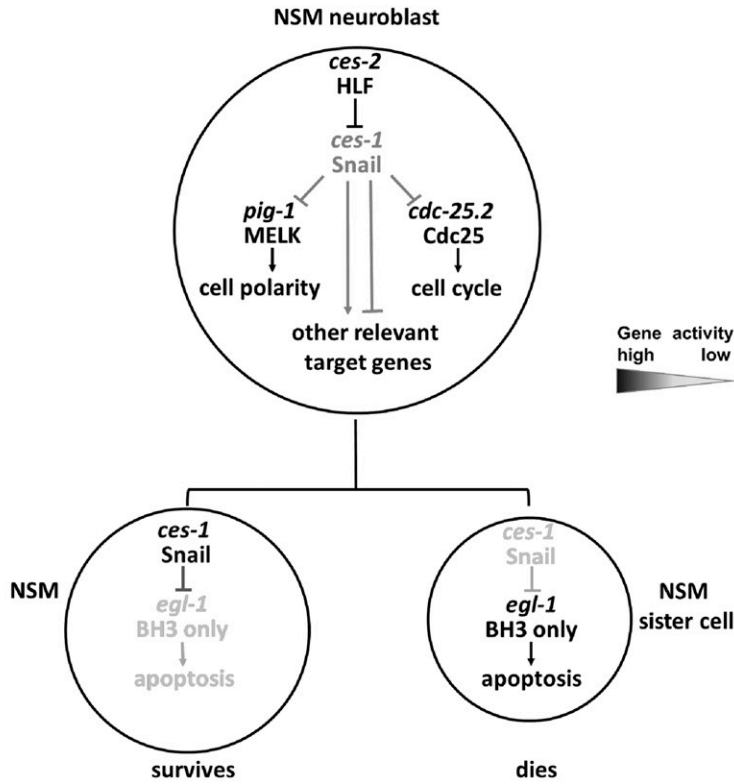
Figure 9 *ces-1* Snail controls the position and orientation of the NSMnb cleavage plane by repressing the expression of *pig-1* MELK. (A) Genetic model of the functions of *ces-1* Snail in the NSM lineage in wild type. See text for details. (B) Schematics of NSMnb division and fate of the NSM and NSMsc in wild type (+/+), *ces-1* gain of function or *ces-2* loss of function, and *pig-1* loss of function. The red dotted lines in the NSMnb indicate the position and orientation of the cleavage plane. See text for details.
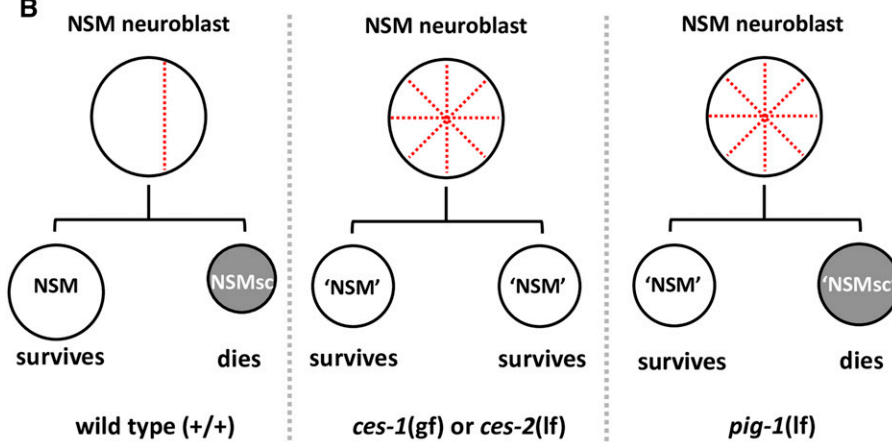
homologs of mammalian LKB1, STRAD, and MO25 (Denning *et al.* 2012; Chien *et al.* 2013; Hirose and Horvitz 2013; Pacquelet *et al.* 2015). Our results indicate that CES-1 Snail-dependent control of *pig-1* MELK expression contributes to the regulation of PIG-1 MELK activity in the NSMnb and that small changes in expression level (~20% more or less) have phenotypic consequences. In support of the notion that control of expression is a mechanism through which the activities of MELK-like kinases are regulated, in the Q.a/p neuroblast, *pig-1* MELK expression is under the control of the Storkhead-box protein 1-like transcription factor HAM-1, whose loss also affects asymmetric cell division in this lineage (Guenther and Garriga 1996; Feng *et al.* 2013). Therefore, we speculate that transcriptional control of MELK genes may be relevant in vertebrates as well and that Snail-

and Storkhead-box protein 1-like transcription factors might contribute to this process.

How does pig-1 MELK affect the position and orientation of the NSMnb cleavage plane?

In the *C. elegans* one-cell embryo, the loss of *pig-1* MELK synergizes with the loss of *ani-1* [which encodes one of two *C. elegans* anillins (Maddox *et al.* 2005)] to cause a defect in the position of the cleavage plane (Pacquelet *et al.* 2015). In this context, PIG-1 and ANI-1 may affect cleavage plane position by regulating the accumulation of myosin at the cell cortex (Pacquelet *et al.* 2015). Indeed, in early embryos, PIG-1 MELK protein has been shown to localize to the cell cortex between adjacent cells. However, in the dividing Q.a/p neuroblasts, which like the NSM neuroblasts divide asymmetrically

to give rise to a daughter that is programmed to die, PIG-1 seems to localize to the two centrosomes (Chien *et al.* 2013). This suggests that in neuroblasts, PIG-1 MELK most likely acts through a mechanism that differs from that in the early embryo. Furthermore, we have recently shown that certain aspects of the polarization of the NSMnb, such as the generation at metaphase of a gradient of apoptotic potential (*i.e.*, active CED-3 caspase), depend on the activity of the central *C. elegans* cell death pathway as well as the two parallel partially redundant *C. elegans* engulfment pathways (Chakraborty *et al.* 2015; Conradt *et al.* 2016; Lambie and Conradt 2016). How a *pig-1* MELK-dependent pathway may intersect with these pathways to cause the asymmetric division of the NSMnb is currently unknown.

Relevance for stem cells and tumorigenesis

Snail-like transcription factors affect various aspects of stem cell function such as self-renewal (Guo *et al.* 2012; Desgrosellier *et al.* 2014; Hwang *et al.* 2014; Lin *et al.* 2014; Horvay *et al.* 2015; Ye *et al.* 2015; Tang *et al.* 2016). In order to self-renew, stem cells need to divide asymmetrically and give rise to two daughters of different fates. Interestingly, at least in mouse and in the zebrafish, the MELK gene is expressed in stem cells, such as neural and hematopoietic stem cells (Nakano *et al.* 2005; Saito *et al.* 2005, 2012). Furthermore, there is increasing evidence (including the evidence presented here) that MELK proteins play a critical role in asymmetric cell division and that their loss or overexpression causes cells that normally divide asymmetrically to divide symmetrically instead (Cordes *et al.* 2006; Tassan 2011; Pacquelet *et al.* 2015). Therefore, we speculate that Snail-like transcription factors are critical for self-renewal because they control MELK expression in stem cell lineages and, hence, the function of MELK in asymmetric cell division.

In some stem cell lineages, Snail-like transcription factors, however, have also been shown to promote the acquisition of a differentiated state (Lin *et al.* 2014; Horvay *et al.* 2015; Tang *et al.* 2016). Studies of CES-1 Snail in the NSM neuroblast lineage may provide a framework for how this could be accomplished mechanistically. In the NSM neuroblast lineage, CES-1 Snail coordinates cell cycle progression and cell polarity in the NSMnb and thereby enables this neuroblast to divide asymmetrically (Hatzold and Conradt 2008; Yan *et al.* 2013). Immediately after NSMnb division, in contrast, CES-1 Snail is critical for cell fate specification and the acquisition of a differentiated state: its absence in the NSMsc causes the NSMsc to acquire the cell death fate and its presence in the NSM allows the NSM to acquire a neuronal fate (Ellis and Horvitz 1991; Thellmann *et al.* 2003; Hatzold and Conradt 2008). The different functions of CES-1 Snail in the NSMnb and its daughter cells can be explained by differences in CES-1 Snail abundance: CES-1 Snail protein is present at a low, undetectable level in the NSMnb and this low level may be necessary and sufficient to control the transcription of *pig-1* MELK and *cdc-25.2* CDC25. Immediately after NSMnb division, this level is increased to a detectable level in the NSM and probably decreased to an even lower level in the NSMsc

(Hatzold and Conradt 2008). Therefore, a level sufficient for transcriptional repression of *egl-1* BH3-only is reached in the NSM but not the NSMsc. [Indeed, the *cis*-acting element of the *egl-1* BH3-only locus necessary for CES-1 Snail-dependent repression contains four Snail binding sites to which CES-1 protein binds in a cooperative manner, at least *in vitro* (Thellmann *et al.* 2003).] By analogy to the *C. elegans* NSM neuroblast lineage, we speculate that the concentrations and, hence, target genes of Snail-like transcription factors in stem cell lineages may change during asymmetric stem cell divisions to promote self-renewal in stem cells, and cell fate specification and terminal differentiation in the nonstem cell daughter.

Finally, the deregulation of both Snail-like transcription factors and MELK has been implicated in tumorigenesis in numerous types of cancers and may even play a central role in cancer stem cells (Puisieux *et al.* 2014; Ganguly *et al.* 2015). Based on our findings in *C. elegans*, we speculate that the deregulation of Snail-like transcription factors or MELK results in the inability of stem cells to divide asymmetrically, and that this loss of self-renewal is a crucial step in tumorigenesis.

Literature Cited

Alessi, D. R., K. Sakamoto, and J. R. Bayascas, 2006 LKB1-dependent signaling pathways. Annu. Rev. Biochem. 75: 137–163.

Audhya, A., F. Hyndman, I. X. McLeod, A. S. Maddox, J. R. Yates, III *et al.*, 2005 A complex containing the Sm protein CAR-1 and the RNA helicase CGH-1 is required for embryonic cytokinesis in Caenorhabditis elegans. J. Cell Biol. 171: 267–279.

Bailey, T. L., M. Boden, F. A. Buske, M. Frith, C. E. Grant *et al.*, 2009 MEME SUITE: tools for motif discovery and searching. Nucleic Acids Res. 37: W202–W208.

Barrallo-Gimeno, A., and M. A. Nieto, 2009 Evolutionary history of the Snail/Scratch superfamily. Trends Genet. 25: 248–252.

Brenner, S., 1974 The genetics of Caenorhabditis elegans. Genetics 77: 71–94.

Chakraborty, S., E. J. Lambie, S. Bindu, T. Mikeladze-Dvali, and B. Conradt, 2015 Engulfment pathways promote programmed cell death by enhancing the unequal segregation of apoptotic potential. Nat. Commun. 6: 10126.

Chien, S. C., E. M. Brinkmann, J. Teuliere, and G. Garriga, 2013 Caenorhabditis elegans PIG-1/MELK acts in a conserved

PAR-4/LKB1 polarity pathway to promote asymmetric neuroblast divisions. Genetics 193: 897–909.

Conradt, B., and H. R. Horvitz, 1998   The C. elegans protein EGL-1 is required for programmed cell death and interacts with the Bcl-2-like protein CED-9. Cell 93: 519–529.

Conradt, B., Y. C. Wu, and D. Xue, 2016   Programmed cell death during Caenorhabditis elegans. Dev. Genet. 203: 1533–1562.

Cordes, S., C. A. Frank, and G. Garriga, 2006   The C. elegans MELK ortholog PIG-1 regulates cell size asymmetry and daughter cell fate in asymmetric neuroblast divisions. Development 133: 2747–2756.

Denning, D. P., V. Hatch, and H. R. Horvitz, 2012   Programmed elimination of cells by caspase-independent cell extrusion in C. elegans. Nature 488: 226–230.

Desgrosellier, J. S., J. Lesperance, L. Seguin, M. Gozo, S. Kato et al., 2014   Integrin alphavbeta3 drives slug activation and stemness in the pregnant and neoplastic mammary gland. Dev. Cell 30: 295–308.

Ellis, R. E., and H. R. Horvitz, 1991   Two C. elegans genes control the programmed deaths of specific cells in the pharynx. Development 112: 591–603.

Feng, G., P. Yi, Y. Yang, Y. Chai, D. Tian et al., 2013   Developmental stage-dependent transcriptional regulatory pathways control neuroblast lineage progression. Development 140: 3838–3847.

Frokjaer-Jensen, C., M. W. Davis, M. Ailion, and E. M. Jorgensen, 2012   Improved Mos1-mediated transgenesis in C. elegans. Nat. Methods 9: 117–118.

Frokjaer-Jensen, C., M. W. Davis, M. Sarov, J. Taylor, S. Flibotte et al., 2014   Random and targeted transgene insertion in Caenorhabditis elegans using a modified Mos1 transposon. Nat. Methods 11: 529–534.

Ganguly, R., A. Mohyeldin, J. Thiel, H. I. Kornblum, M. Beullens et al., 2015   MELK-a conserved kinase: functions, signaling, cancer, and controversy. Clin. Transl. Med. 4: 11.

Gerstein, M. B., Z. J. Lu, E. L. Van Nostrand, C. Cheng, B. I. Arshinoff et al., 2010   Integrative analysis of the Caenorhabditis elegans genome by the modENCODE project. Science 330: 1775–1787.

Gladden, J. M., and B. J. Meyer, 2007   A ONECUT homeodomain protein communicates X chromosome dose to specify Caenorhabditis elegans sexual fate by repressing a sex switch gene. Genetics 177: 1621–1637.

Guenther, C., and G. Garriga, 1996   Asymmetric distribution of the C. elegans HAM-1 protein in neuroblasts enables daughter cells to adopt distinct fates. Development 122: 3509–3518.

Guo, W., Z. Keckesova, J. L. Donaher, T. Shibue, V. Tischler et al., 2012   Slug and Sox9 cooperatively determine the mammary stem cell state. Cell 148: 1015–1028.

Hatzold, J., and B. Conradt, 2008   Control of apoptosis by asymmetric cell division. PLoS Biol. 6: e84.

Hirose, T., and H. R. Horvitz, 2013   An Sp1 transcription factor coordinates caspase-dependent and -independent apoptotic pathways. Nature 500: 354–358.

Horner, M. A., S. Quintin, M. E. Domeier, J. Kimble, M. Labouesse et al., 1998   pha-4, an HNF-3 homolog, specifies pharyngeal organ identity in Caenorhabditis elegans. Genes Dev. 12: 1947–1952.

Horvay, K., T. Jarde, F. Casagranda, V. M. Perreau, K. Haigh et al., 2015   Snai1 regulates cell lineage allocation and stem cell maintenance in the mouse intestinal epithelium. EMBO J. 34: 1319–1335.

Huang da, W., B. T. Sherman, and R. A. Lempicki, 2009   Systematic and integrative analysis of large gene lists using DAVID bioinformatics resources. Nat. Protoc. 4: 44–57.

Hwang, W. L., J. K. Jiang, S. H. Yang, T. S. Huang, H. Y. Lan et al., 2014   MicroRNA-146a directs the symmetric division of Snail-dominant colorectal cancer stem cells. Nat. Cell Biol. 16: 268–280.

Kim, J., I. Kawasaki, and Y. H. Shim, 2010   cdc-25.2, a C. elegans ortholog of cdc25, is required to promote oocyte maturation. J. Cell Sci. 123: 993–1000.

Lambie, E. J., and B. Conradt, 2016   Deadly dowry: how engulfment pathways promote cell killing. Cell Death Differ. 23: 553–554.

Landt, S. G., G. K. Marinov, A. Kundaje, P. Kheradpour, F. Pauli et al., 2012   ChIP-seq guidelines and practices of the ENCODE and modENCODE consortia. Genome Res. 22: 1813–1831.

Langmead, B., and S. L. Salzberg, 2012   Fast gapped-read alignment with Bowtie 2. Nat. Methods 9: 357–359.

Li, Q. H., J. B. Brown, H. Y. Huang, and P. J. Bickel, 2011   Measuring reproducibility of high-throughput experiments. Ann. Appl. Stat. 5: 1752–1779.

Lin, Y., X. Y. Li, A. L. Willis, C. Liu, G. Chen et al., 2014   Snail1-dependent control of embryonic stem cell pluripotency and lineage commitment. Nat. Commun. 5: 3070.

Lizcano, J. M., O. Goransson, R. Toth, M. Deak, N. A. Morrice et al., 2004   LKB1 is a master kinase that activates 13 kinases of the AMPK subfamily, including MARK/PAR-1. EMBO J. 23: 833–843.

Maddox, A. S., B. Habermann, A. Desai, and K. Oegema, 2005   Distinct roles for two C. elegans anillins in the gonad and early embryo. Development 132: 2837–2848.

Melendez, A., and I. Greenwald, 2000   Caenorhabditis elegans lin-13, a member of the LIN-35 Rb class of genes involved in vulval development, encodes a protein with zinc fingers and an LXCXE motif. Genetics 155: 1127–1137.

Mello, C., and A. Fire, 1995   DNA transformation. Methods Cell Biol. 48: 451–482.

Metzstein, M. M., and H. R. Horvitz, 1999   The C. elegans cell death specification gene ces-1 encodes a snail family zinc finger protein. Mol. Cell 4: 309–319.

Metzstein, M. M., M. O. Hengartner, N. Tsung, R. E. Ellis, and H. R. Horvitz, 1996   Transcriptional regulator of programmed cell death encoded by Caenorhabditis elegans gene ces-2. Nature 382: 545–547.

Nakano, I., A. A. Paucar, R. Bajpai, J. D. Dougherty, A. Zewail et al., 2005   Maternal embryonic leucine zipper kinase (MELK) regulates multipotent neural progenitor proliferation. J. Cell Biol. 170: 413–427.

Narasimhan, K., S. A. Lambert, A. W. Yang, J. Riddell, S. Mnaimneh et al., 2015   Mapping and analysis of Caenorhabditis elegans transcription factor sequence specificities. ELife 4: 06967.

Nieto, M. A., R. Y. Huang, R. A. Jackson, and J. P. Thiery, 2016   Emt: 2016. Cell 166: 21–45.

Pacquelet, A., P. Uhart, J. P. Tassan, and G. Michaux, 2015   PAR-4 and anillin regulate myosin to coordinate spindle and furrow position during asymmetric division. J. Cell Biol. 210: 1085–1099.

Puisieux, A., T. Brabletz, and J. Caramel, 2014   Oncogenic roles of EMT-inducing transcription factors. Nat. Cell Biol. 16: 488–494.

Reece-Hoyes, J. S., B. Deplancke, M. I. Barrasa, J. Hatzold, R. B. Smit et al., 2009   The C. elegans Snail homolog CES-1 can activate gene expression in vivo and share targets with bHLH transcription factors. Nucleic Acids Res. 37: 3689–3698.

Reinke, V., M. Krause, and P. Okkema, 2013   Transcriptional regulation of gene expression in C. elegans. WormBook, ed. The C. elegans Research Community, WormBook, doi/10.1895/wormbook.1.45.2, http://www.wormbook.org

Rembold, M., L. Ciglar, J. O. Yanez-Cuna, R. P. Zinzen, C. Girardot et al., 2014   A conserved role for Snail as a potentiator of active transcription. Genes Dev. 28: 167–181.

Robinson, J. T., H. Thorvaldsdottir, W. Winckler, M. Guttman, E. S. Lander et al., 2011   Integrative genomics viewer. Nat. Biotechnol. 29: 24–26.

Saito, R., Y. Tabata, A. Muto, K. Arai, and S. Watanabe, 2005   Melk-like kinase plays a role in hematopoiesis in the zebra fish. Mol. Cell. Biol. 25: 6682–6693.

Saito, R., H. Nakauchi, and S. Watanabe, 2012   Serine/threonine kinase, Melk, regulates proliferation and glial differentiation of retinal progenitor cells. Cancer Sci. 103: 42–49.

Sarov, M., S. Schneider, A. Pozniakovski, A. Roguev, S. Ernst *et al.*, 2006   A recombineering pipeline for functional genomics applied to Caenorhabditis elegans. Nat. Methods 3: 839–844.

Sarov, M., J. I. Murray, K. Schanze, A. Pozniakovski, W. Niu *et al.*, 2012   A genome-scale resource for in vivo tag-based protein function exploration in C. elegans. Cell 150: 855–866.

Sulston, J. E., E. Schierenberg, J. G. White, and J. N. Thomson, 1983   The embryonic cell lineage of the nematode Caenorhabditis elegans. Dev. Biol. 100: 64–119.

Tang, Y., T. Feinberg, E. T. Keller, X. Y. Li, and S. J. Weiss, 2016   Snail/Slug binding interactions with YAP/TAZ control skeletal stem cell self-renewal and differentiation. Nat. Cell Biol. 18: 917–929.

Tassan, J. P., 2011   Cortical localization of maternal embryonic leucine zipper kinase (MELK) implicated in cytokinesis in early xenopus embryos. Commun. Integr. Biol. 4: 483–485.

Thellmann, M., J. Hatzold, and B. Conradt, 2003   The Snail-like CES-1 protein of C. elegans can block the expression of the BH3-only cell-death activator gene egl-1 by antagonizing the function of bHLH proteins. Development 130: 4057–4071.

Woodruff, J. B., O. Wueseke, V. Viscardi, J. Mahamid, S. D. Ochoa *et al.*, 2015   Centrosomes. Regulated assembly of a supramolecular centrosome scaffold in vitro. Science 348: 808–812.

Yan, B., N. Memar, J. Gallinger, and B. Conradt, 2013   Coordination of cell proliferation and cell fate determination by CES-1 snail. PLoS Genet. 9: e1003884.

Ye, X., W. L. Tam, T. Shibue, Y. Kaygusuz, F. Reinhardt *et al.*, 2015   Distinct EMT programs control normal mammary stem cells and tumour-initiating cells. Nature 525: 256–260.

Zeitlinger, J., R. P. Zinzen, A. Stark, M. Kellis, H. Zhang *et al.*, 2007   Whole-genome ChIP-chip analysis of Dorsal, Twist, and Snail suggests integration of diverse patterning processes in the Drosophila embryo. Genes Dev. 21: 385–390.

Zhang, Y., T. Liu, C. A. Meyer, J. Eeckhoute, D. S. Johnson *et al.*, 2008   Model-based analysis of ChIP-Seq (MACS). Genome Biol. 9: R137.

Zhong, M., W. Niu, Z. J. Lu, M. Sarov, J. I. Murray *et al.*, 2010   Genome-wide identification of binding sites defines distinct functions for Caenorhabditis elegans PHA-4/FOXA in development and environmental response. PLoS Genet. 6: e1000848.

Communicating editor: O. Hobert